SUPPLEMENTARY DATA

Microglia undergo molecular and functional adaptations to dark and light phases in male laboratory mice

Daniele Mattei[1,2,*,§], Andranik Ivanov[3,*], Jacqueline Hammer[4,*], Bilge Ugursu[5,6,7], Sina Schalbetter[1], Juliet Richetto[1], Ulrike Weber-Stadelbauer[1], Flavia Mueller[1], Joseph Scarborough[1], Susanne A Wolf[5,6,7], Helmut Kettenmann[5,8], Bernd Wollscheid[4], Dieter Beule[3], Urs Meyer[1,9,§]

[1] Institute of Pharmacology and Toxicology, University of Zurich-Vetsuisse, Zurich, Switzerland.
[2] Nash Family Department of Neuroscience & Friedman Brain Institute, Icahn School of Medicine at Mount Sinai, New York, NY, United States of America.
[3] Core Unit Bioinformatics, Berlin Institute of Health, Charité-Universitätsmedizin, Berlin, Germany.
[4] Institute of Molecular Systems Biology and Department for Health Sciences and Technology, ETH Zürich, Switzerland.
[5] Cellular Neuroscience, Max-Delbrueck-Center for Molecular Medicine in the Helmholtz Association, Berlin, Germany.
[6] Department of Ophthalmology, Charité – Universitätsmedizin Berlin, Germany.
[7] Psychoneuroimmunology, Max-Delbrueck-Center for Molecular Medicine in the Helmholtz Association, Berlin, Germany.
[8] Shenzhen Institute of Advanced Technology, Chinese Academy of Sciences, Shenzhen, China.
[9] Neuroscience Center Zurich, University of Zurich and ETH Zurich, Zurich, Switzerland.

* The first three authors contributed equally.
§ Corresponding authors at the Nash Family Department of Neuroscience & Friedman Brain Institute, Icahn School of Medicine at Mount Sinai, New York, NY, United States of America (D. Mattei: daniele.mattei@mssm.edu) or Institute of Pharmacology and Toxicology, University of Zurich-Vetsuisse, 8057 Zurich, Switzerland (U. Meyer: urs.meyer@vetpharm.uzh.ch)

Supplementary Figures

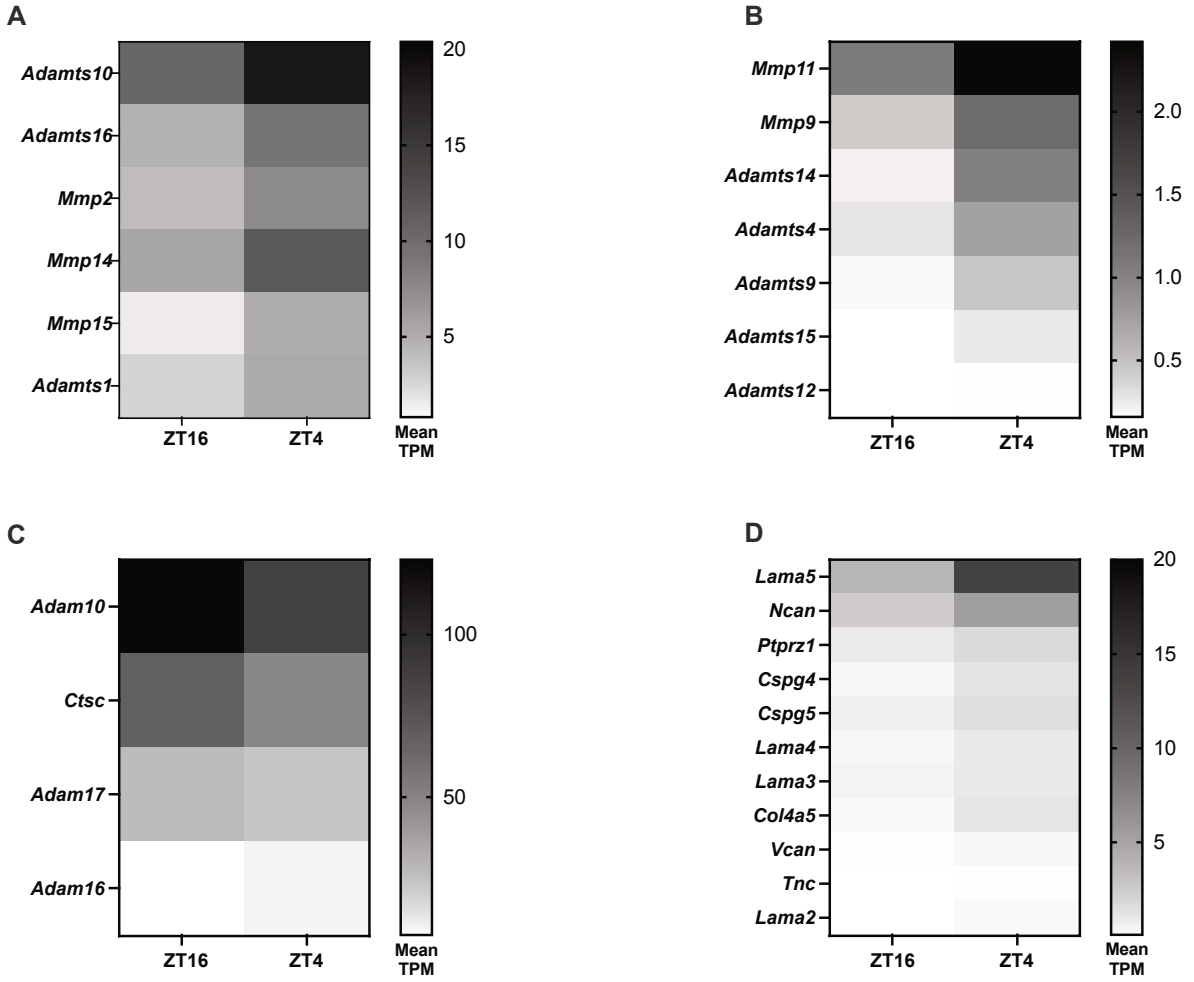

Supplementary Figure S1. A-D Heatmaps displaying the changes in average transcripts per million (TPM) for genes coding for enzyme dedicated to the extracellular matrix (ECM) breakdown **A-C** and genes coding for ECM components **D** in the microglial transcriptional comparison between ZT4 (light phase) and ZT16 (dark phase). Genes that were significantly differentially expressed are displayed (adj. $p < 0.05$).

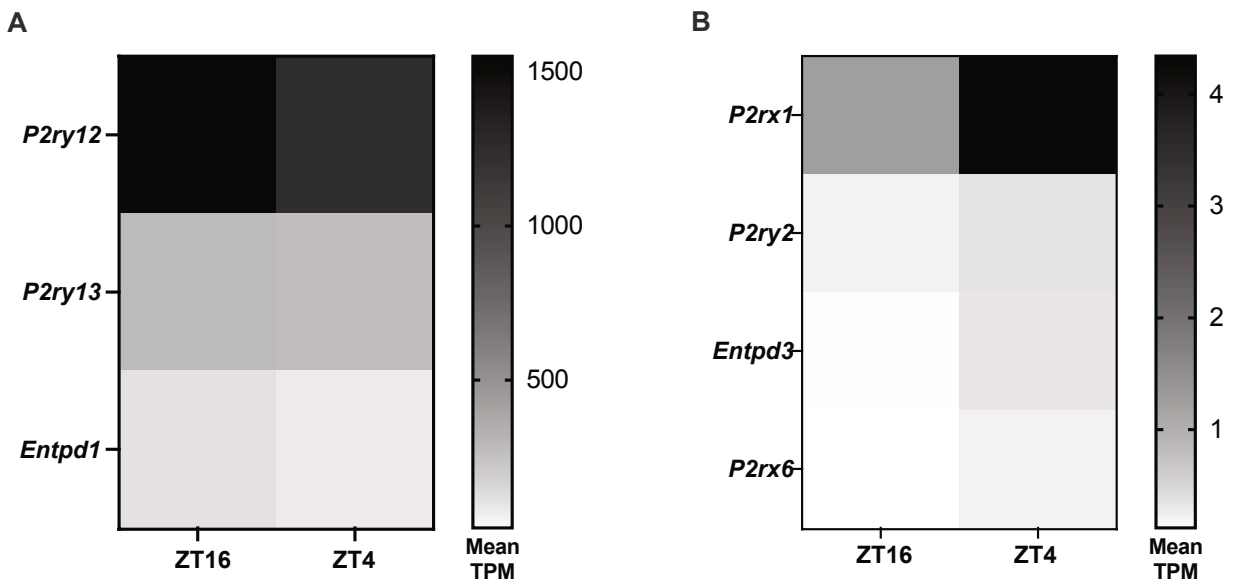

Supplementary Figure S2. Heatmaps displaying the changes in average transcripts per million (TPM) for highly **A** and lowly **B** expressed genes coding for purinergic receptors and enzymes involved in the breakdown of extracellular nucleotides in the microglial transcriptional comparison between ZT4 (light phase) and ZT16 (dark phase). Genes that were significantly differentially expressed are displayed (adj. $p < 0.05$).

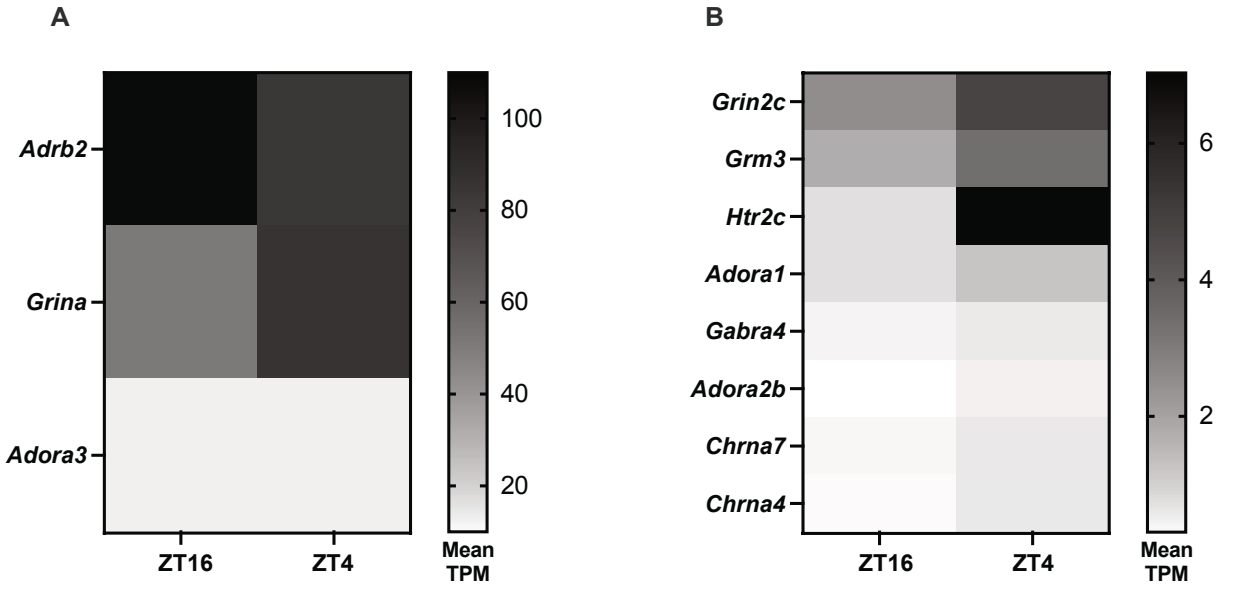

Supplementary Figure S3. Heatmaps displaying the light- and dark-phase associated changes from the microglial transcriptional comparison between ZT4 (light phase) and ZT16 (dark phase), in average transcripts per million (TPM) for highly **A** and lowly **B** expressed genes coding for neurotransmitter receptors. Genes that were significantly differentially expressed are displayed (adj. $p < 0.05$).

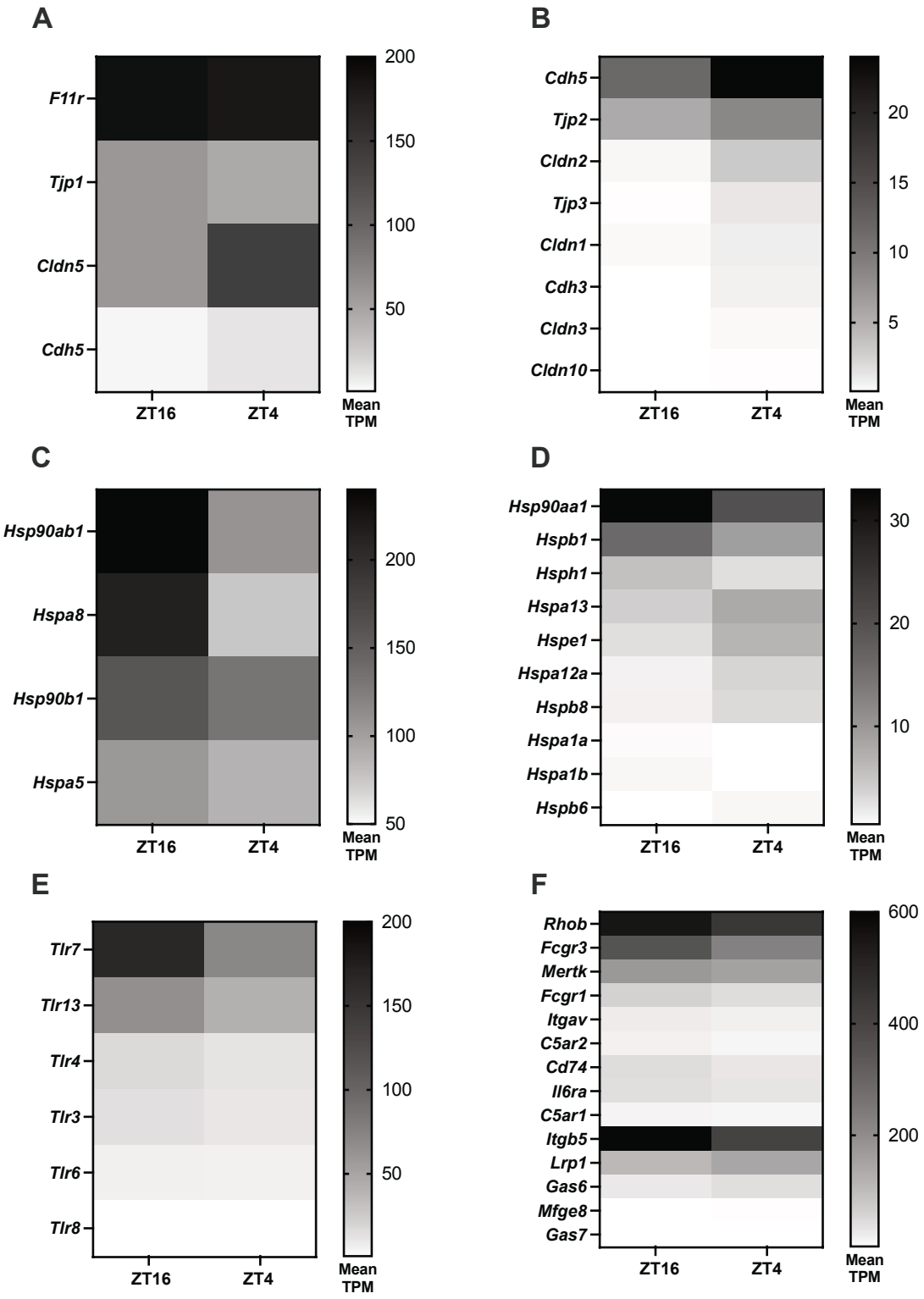

Supplementary Figure S4. Heatmaps showing the differential expression (in average transcripts per million, TPM) for selected genes annotating with cell-to-cell adhesion and junction formation **(A-B)**, heat-shock proteins **(C-D)**, toll-like receptors **(E)**, and genes relevant for microglial activation and phagocytosis **(F)**. Only genes with significant differential expression (adj. $p < 0.05$), as analyzed using total-RNA-seq of hippocampal microglia collected at ZT16 or ZT4 are shown.

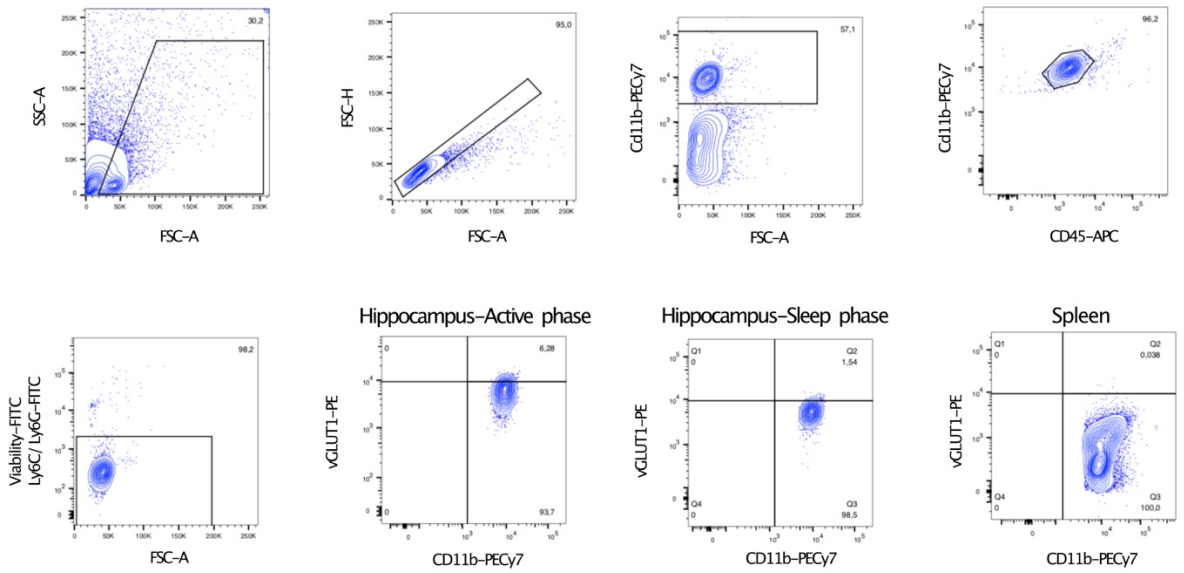

Supplementary Figure S5. Gating strategy for the flow cytometry analysis of vGLUT1-positive inclusions within hippocampal microglia cells sorted during wither the active (ZT16) or the sleep phase (ZT4).

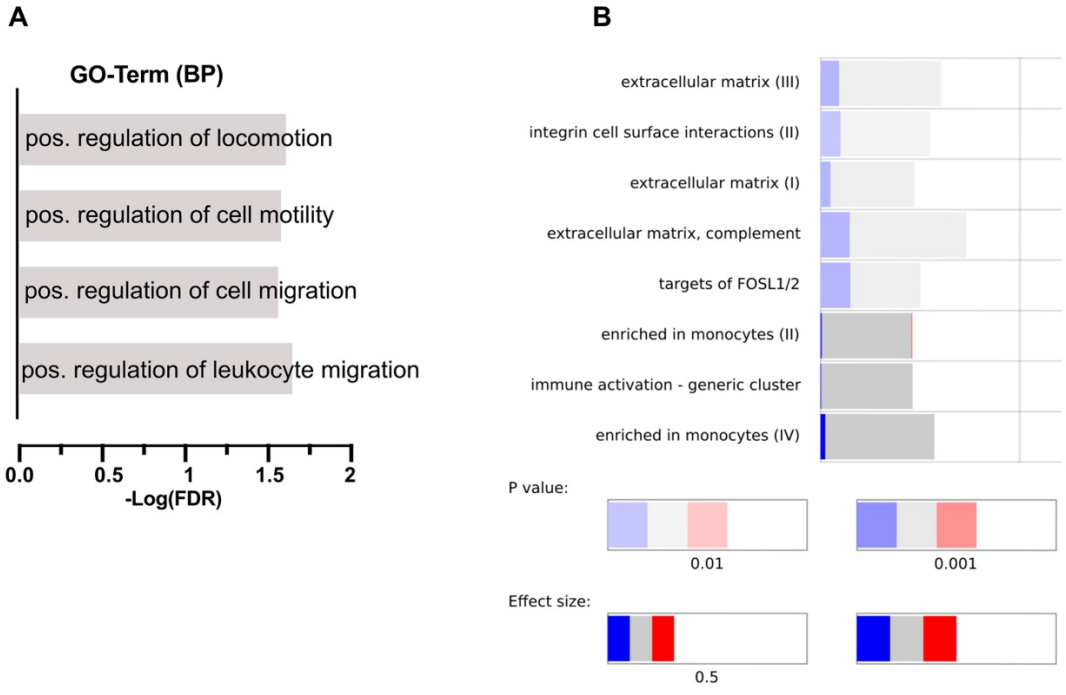

Supplementary Figure S6. (A) -Log(FDR) values for biological processes associated with the genes deregulated in response to LPS as a function of time of injection. **(B)** Unbiased Tmod enrichment analysis for reactome gene sets for the LPS response genes regulated by time of injection.

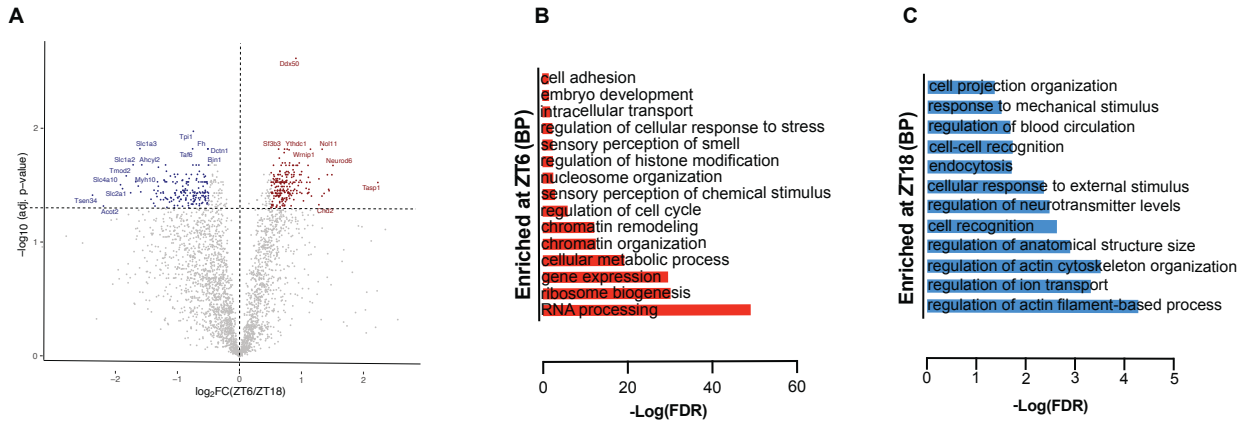

Supplementary Figure S7. Basal differences in the microglial proteome as a function of time-of-sample-collection. **(A)** Volcano plot showing the differentially expressed proteins in hippocampal microglia collected during the sleep phase (ZT6) relative to active phase (ZT18). 481 proteins were found to be differentially regulated between the light and dark phase (adj. $p<$ 0.05, N = 4/group). **B-C** -Log(FDR) values for selected biological processes from the gene ontology analysis of the up- and downregulated proteins between ZT6 and ZT18.

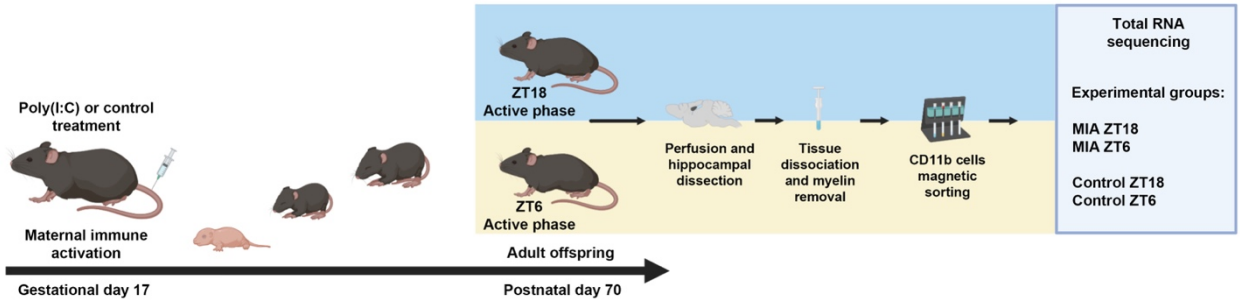

Supplementary Figure S8. Schematic representation of the experimental design used to investigate the influence of time-of-sample-collection on the microglial transcriptome after maternal immune activation (MIA). MIA was induced by treating pregnant dams with poly(I:C) on gestational day 17, whereas control dams received vehicle solution only. Hippocampal microglia were isolated from the hippocampus of adult offspring born to poly(I:C)- or vehicle-exposed dams. Hippocampal microglia were isolated either during the offspring's active phase (ZT18) or sleep phase (ZT6) and subjected to total RNA sequencing (RNAseq).

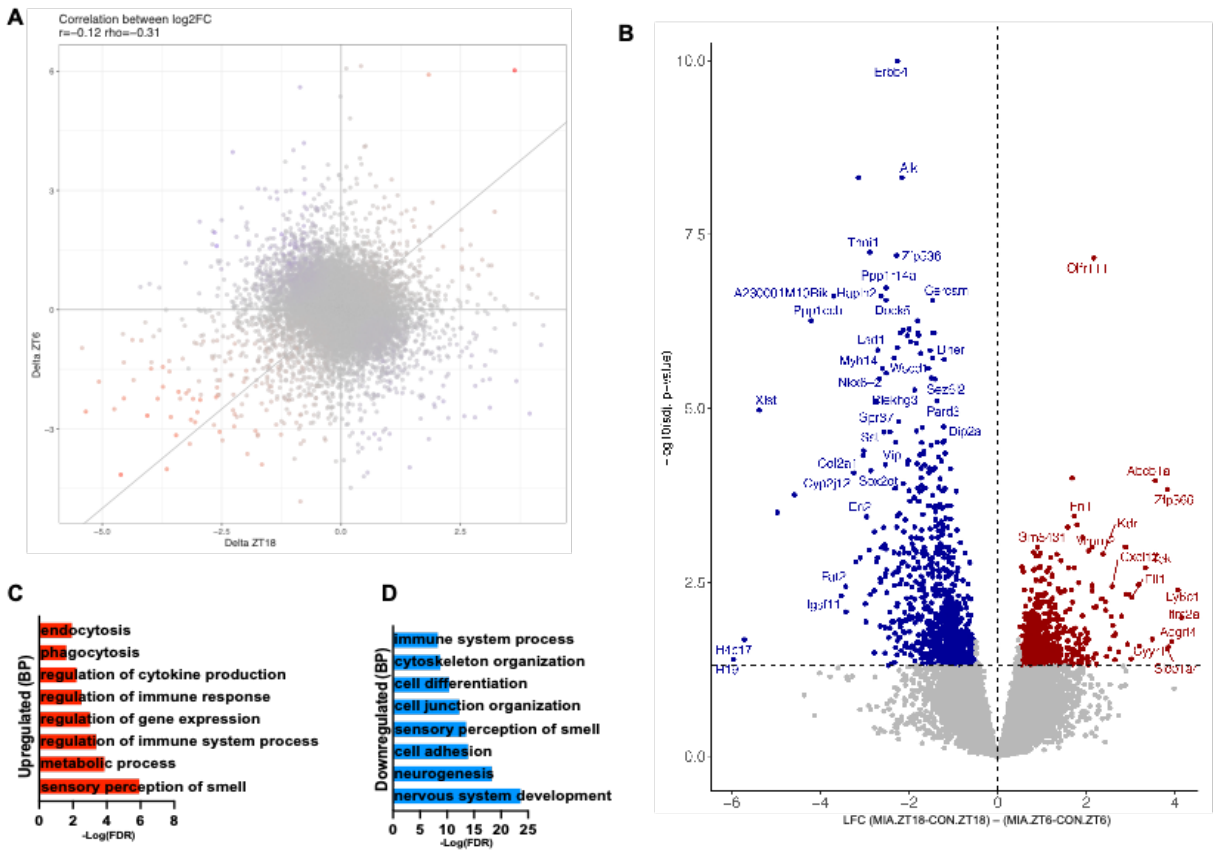

Supplementary Figure S9. The effect of maternal immune activation (MIA) on the transcriptional changes between the light and dark phase in adult MIA offspring. In this additional analysis, the effects of time of sample collection were contrasted by subtracting the relative gene expression changes occurring in MIA compared to control offspring (CON) during the active (dark) phase from the transcriptional changes occurring in MIA compared to CON offspring during the light (sleep) phase. **(A)** Disco plot for the correlation between the absolute Log2-fold changes in gene expression between MIA- and vehicle-exposed offspring subjected to microglia collection during the active phase (x-axis) and sleep phase (y-axis). **(B)** Volcano plot showing genes significantly affected by MIA as a function of the time of sample collection, as analyzed using the delta contrast analysis (Delta = (MIA_ZT18 vs. CON_3 ZT18)-(MIA_ZT6 vs. CON_ZT6). (C) -Log(FDR) values for selected biological processes (BPs) found to be up- or downregulated between the active and sleep phase after MIA.

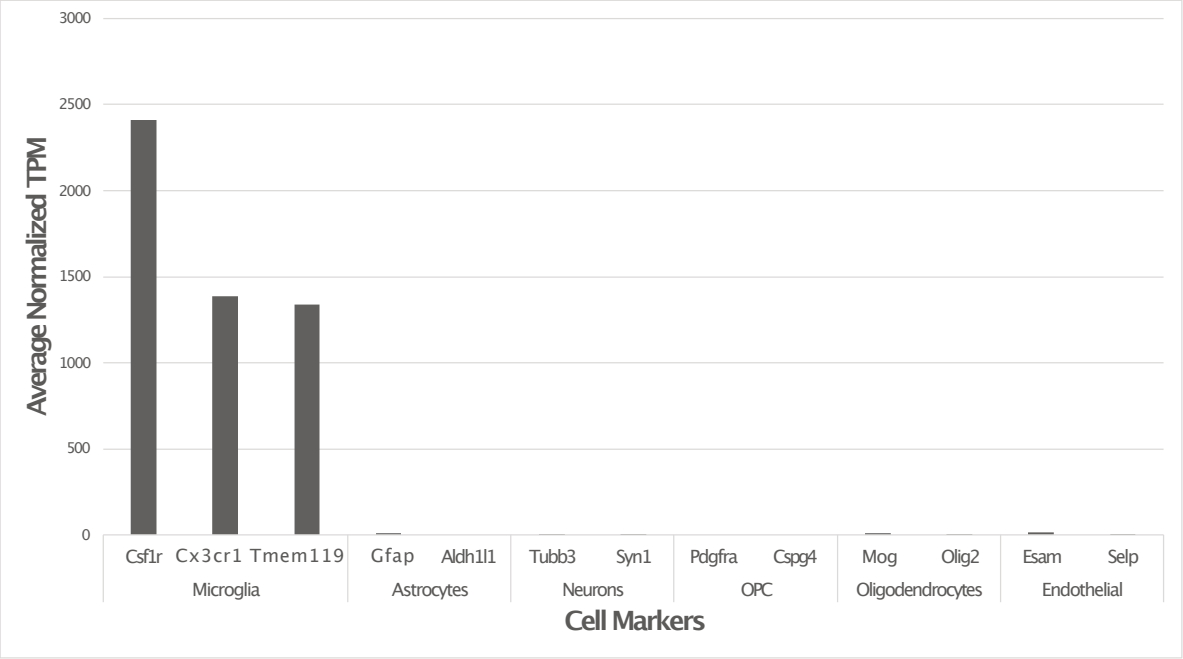

Supplementary Figure S10. Bar graph showing the enrichment in microglia cells following CD11b MACS sorting, by comparison of the expression level of canonical microglial markers *Csf1r, Cx3cr1* and *Tmem119* to non-microglial cell markers. The normalized transcripts per million (TPM) values (X-axis) for each gene were averaged across the sorted batches.

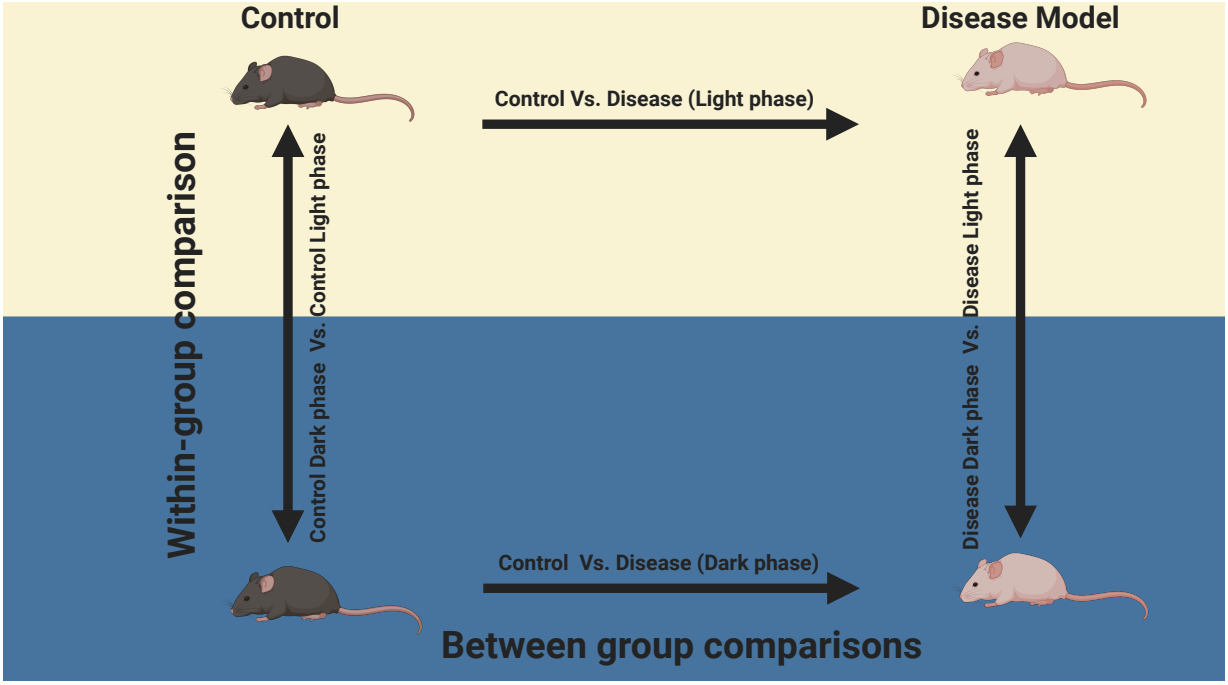

Supplementary Figure S11. Schematic representation of the experimental design used in the present study to investigate the microglial dynamics between the light and dark phases in physiology (control conditions) and in pathophysiology (disease model). As displayed in the cartoon, the design includes within- and between group comparisons of microglial readouts encompassing both the light and dark phases. This design ensures a more comprehensive study of microglia cells diurnal dynamics in physiology (control group comparisons) and in pathophysiology (disease model comparisons). Images were created with Biorender.com.

Supplementary Tables

All supplementary tables (Supplementary Tables S1-S7) are provided as separate documents. The corresponding figure legends are provided below.

Table S1: Complete table for the differentially expressed microglial genes (DEGs) between ZT4 and ZT16, followed by gene ontology terms for biological processes associated with the DEGs. All genes differentially expressed (adj. $p < 0.05$) are included in the table.

Table S2: Table displaying the differential gene expression of selected homeostatic and disease-associated microglial (DAMs) genes between ZT4 and ZT16. Positive Log2FCs indicate an enrichment in the sleep phase, negative Log2FCs indicate an enrichment in the active phase.

Table S3: Complete table for the differentially expressed microglial genes and proteins in response to LPS at ZT18. (active phase) and ZT6 (sleep phase), followed by gene ontology terms for biological processes associated with the deregulated genes and proteins in each condition. All genes differentially expressed (adj. $p < 0.05$) are included in the table.

Table S4: Complete table for the differentially expressed microglial proteins between ZT18 (active phase) and ZT6 (sleep phase) followed by gene ontology terms for biological processes associated with the differentially expressed proteins (adj. $p < 0.05$). Positive Log2FCs indicate an enrichment in the sleep phase, negative Log2FCs indicate an enrichment in the active phase.

Table S5: Table showing transcriptional and proteotype changes in genes and proteins relevant for microglial mitochondrial and metabolic functions, immune activation, motility, and phagocytosis, and chromatin remodeling. Displayed are the Log2 fold changes (Log2FC) and adjusted *p*-values for the differential gene expression between ZT4 and ZT16 followed by the changes in protein expression between ZT6 and ZT18. Positive Log2FCs indicate an enrichment in the sleep phase, negative Log2FCs indicate an enrichment in the active phase.

Table S6: Table showing transcriptional and proteotype changes between ZT6 and ZT18 in genes and proteins responsible for the epigenetic remodeling of chromatin accessibility at baseline (green) and in response to LPS at either ZT18 (orange) or ZT6 (blue). Displayed are the Log2 fold changes (Log2FC) and for the differential gene/protein expression between ZTZ6 and ZT18. Positive Log2FCs indicate an enrichment in the sleep phase, negative Log2FCs indicate an enrichment in the active phase.

Table S7: Complete table for the differentially expressed microglial genes between the active (ZT18) and sleep (ZT6) phases in adult offspring exposed to poly(I:C)-based maternal immune activation (MIA) relative to vehicle-treated control offspring. The table also summarizes the gene ontology terms for biological processes associated with the differentially expressed genes in each condition.
